Calcium dependence of aequorin bioluminescence dissected by random mutagenesis

L. Tricoire, K. Tsuzuki, O. Courjean, N. Gibelin, G. Bourout, J. Rossier, B. Lambolez

PNAS, 2006 , June 26, 103 (25), 9500-9505

BIOLOGICAL SCIENCES
Biochemistry

Calcium dependence of aequorin bioluminescence dissected by random mutagenesis

Ludovic Tricoire*, Keisuke Tsuzuki*, Olivier Courjean, Nathalie Gibelin, Gaëlle Bourout, Jean Rossier and Bertrand Lambolez.

Laboratoire de Neurobiologie et Diversité Cellulaire, CNRS UMR 7637, Ecole Supérieure de Physique et de Chimie Industrielles, 10 rue Vauquelin, 75005 Paris, France.

** equal first authors*

Corresponding author: Bertrand Lambolez, NPA, CNRS UMR 7102, UPMC, 9 quai St Bernard 75005 Paris, France. Telephone: (33 1) 44 27 25 09. Facsimile: (33 1) 44 27 25 84. E-mail: bertrand.lambolez@snv.jussieu.fr

Text: 14 pages - Figures: 5 – Abstract: 208 words – Total characters: 46824

Abbreviations: WT: wild type

ABSTRACT

Aequorin bioluminescence is emitted as a rapidly decaying flash upon calcium binding. Random mutagenesis and functional screening were used to isolate aequorin mutants showing slow decay rate of luminescence. Calcium sensitivity curves were shifted in all mutants, and an intrinsic link between calcium sensitivity and decay rate was suggested by the position of all mutations in or near EF-hand calcium binding sites. From these results, a low calcium affinity was assigned to the N-terminal EF-hand and a high affinity to the C-terminal EF-hand pair. In wild-type aequorin, the increase of the decay rate with calcium occurred at constant total photon yield, and thus determined a corresponding increase of light intensity. Increase of the decay rate was underlain by variations of a fast and a slow component and required the contribution of all three EF-hands. Conversely, analyses of double EF-hand mutants suggested that single EF-hands are sufficient to trigger luminescence at a slow rate. Finally, a model postulating that proportions of a fast and a slow light-emitting state depend on calcium concentration adequately described the calcium dependence of aequorin bioluminescence. Our results suggest that variations of luminescence kinetics, which depend on three EF-hands endowed with different calcium affinities, critically determine the amplitude of aequorin responses to biological calcium signals.

INTRODUCTION

The photoprotein aequorin is a stable luciferase intermediate formed from the reaction of the protein apoaequorin (luciferase) and the substrate coelenterazine (luciferin), which emits light upon Ca^{2+} binding (1-5). Aequorin contains three EF-hand Ca^{2+}-binding sites (6-8) located close to its N-terminus (EF1) or its C-terminus (EF2,3 pair). Aequorin mutagenesis and crystal structure suggest that these three EF-hands indeed bind Ca^{2+} but their individual contribution to luminescence is still a matter of debate (9-13).

The steep increase of luminescence intensity with [Ca^{2+}] makes aequorin a useful reporter of intracellular calcium signals (14). The formation of aequorin is a slow process (15), whereas the luminescence reaction is very fast and proceeds to completion in the continuous presence of Ca^{2+}. The aequorin response thus occurs as a flash which decays exponentially and whose onset rate does not depend on [Ca^{2+}] (16). It has been early observed that the decay rate of this response increases with [Ca^{2+}], while the total light emitted (light integral) remains relatively constant (16). This suggests that the increase of luminescence intensity with [Ca^{2+}] is determined by variations of the decay rate, but not of the light integral. In other words, the shorter is the duration of the flash (i.e. the faster is the decay), the larger is the amplitude of the response (i.e. light intensity). However, the relationships between the intensity, the decay rate and the integral of bioluminescence and their links to EF-hand occupancy have not been clearly established.

In order to analyze the contribution of decay kinetics to aequorin responses, we recently isolated aequorin mutants exhibiting slow decay rates (SloDK mutants) through random mutagenesis and functional screening (17). This procedure allows the selection of mutants that most efficiently affect a specific subfunction of a protein with minimal alteration of its overall structure-function relationships. A different screening process yielded other mutants (Bright) exhibiting high luminescence in bacteria due to increased Ca^{2+} sensitivity or photoprotein stability (17). In contrast with SloDK mutants in which both Ca^{2+} sensitivity and decay rate are modified, Bright mutants show modifications of Ca^{2+} sensitivity with little change of decay rate. Both SloDK and Bright mutants carried single aminoacid substitutions located in EF-hands or their adjacent α-helices. Here, the dependence of mutant and WT aequorin luminescence on [Ca^{2+}] was analyzed and combined with modeling to examine the contribution of the three EF-hands and the role of decay kinetics in aequorin responses. We found that EF-hands have different Ca^{2+} affinities and all contribute to the variations of decay rate which determine the increase of luminescence intensity with [Ca^{2+}].

MATERIALS AND METHODS

Cell-free expression of WT and mutant apoproteins was performed as described (17) using the Rapid Translation System (RTS, Roche Diagnostics, Mannheim, Germany) from cDNAs subcloned in the pRSETc expression vector (Invitrogen, Carlsbad, CA). Reactions were diluted 1:1 in glycerol and this working stock was stored at –20°C.

Aequorin was reconstituted for 1 h at 4°C in the presence of 1,4-dithiothreitol, 10 mM; Tris (pH8), 50 mM; EDTA, 10 µM and coelenterazine, 5 µM and then diluted 20 times into Tris (pH8), 50 mM ; EDTA, 10 µM to minimize coelenterazine luminescence background. Fifty µl of this solution (corresponding to 0.2 µl of apoaequorin working stock) was used per well for luminescence assay performed in 96-well plates. Aequorin activity was measured at 22°C in a PhL microplate luminometer (Mediator, Vienna, Austria) by injecting 100 µl of solutions containing Tris (pH8), 50 mM with variable $CaCl_2$ concentrations buffered with EDTA, 10 µM. The free [Ca^{2+}] immediately after mixing were calculated from affinity constants of EDTA using the WebMaxc v2.22 program (http://www.stanford.edu/~cpatton/webmaxcSR.htm, see ref. 18), taking into account 3 µM contaminating Ca^{2+}. Indeed, contaminating [Ca^{2+}] found in a Tris (pH8), 50 mM solution was 3.5 µM, as determined by elemental analysis; or was 3 µM free Ca^{2+}, as measured by fluorescence of the Calcium Green indicator calibrated against the Calcium Calibration Buffer kit (Molecular Probes, Eugene, OR).

Data were collected with 0.1 s integration time. Luminescence exponential decays were analyzed using the Clampfit 8.1 software (Axon instruments, Foster City, CA). Fast and slow components of double exponentials are described by their time constants (τ_F and τ_S, respectively) and their light integrals (Σ_F and Σ_S, respectively), while Σ_T represents the total light integral ($\Sigma_F + \Sigma_S$). In our PhL luminometer, injection of 100 µl solution required 280 ms and recording started 365 ms after the beginning of injection, during the decay phase after luminescence onset (~10ms, see ref. 16). Corrected Σ_T values that appear in the text take into account this 365 ms lag and were calculated from the formula:

$$\Sigma_T = \Sigma_S \, e^{\frac{0.365}{\tau_S}} + \Sigma_F \, e^{\frac{0.365}{\tau_F}}$$

Each value represents the mean of at least 2 experiments performed in triplicate. Results are expressed as mean ± SEM.

RESULTS

Bright and SloDK mutations (17) affect residues conserved in other photoproteins (see supporting information), located either in EF-hands at canonical Ca^{2+} binding positions (8) or in their adjacent α-helices (figure 1A). Each SloDK mutation was selected several times independently during the screening of random mutants (17) and four of them similarly consisted in a D/E to G substitution at an EF-hand border. This suggests that SloDK mutations efficiently affect the decay rate while other aequorin properties remain relatively unaffected. Indeed, the luminescence decay rates of SloDK mutants were strikingly slow, with half-decay times ranging from 20 fold ($F^{149}S$) to 57 fold ($E^{35}G$) greater than that of WT aequorin (figure 1B). In contrast, luminescence half-decay times of Bright mutants were similar to or only slightly slower than WT.

Luminescence intensity

The [Ca^{2+}] dependence of luminescence intensity was first examined. Since in our experimental setup, recording started after the peak of bioluminescence (see methods), curves were plotted from initial maximum intensity measured upon Ca^{2+} addition (figure 2A). The plot of the $L^{170}I$ mutant, very close to that of $Q^{168}R$, was omitted for clarity. EC50s for Ca^{2+} interpolated from these curves (figure 1B) are used as an index of Ca^{2+} sensitivity.

The three mutants of the EF1 region showed a higher sensitivity to Ca^{2+} than WT aequorin. The effect of $N^{26}D$ likely results from an increased EF1 affinity, consistent with the replacement of the polar Ca^{2+} binding asparagine residue by a negatively charged residue. The effect of $E^{35}G$ seems paradoxical, given that this mutation removes an essential Ca^{2+} binding sidechain (8,19). This can be resolved by assuming that EF1 has lower Ca^{2+} affinity than EF2 and EF3, and that $E^{35}G$ impairs EF1 contribution to the response to Ca^{2+}. Similarly, $V^{44}A$ may also impair contribution of EF1 to bioluminescence, thus increasing the relative contribution of the high affinity EF2 and 3. Indeed, V^{44} interacts with the A^{40} coelenterazine binding residue (11).

Mutants of the EF2 and 3 domains exhibited a lower Ca^{2+} sensitivity than WT aequorin. The effects of $D^{117}G$, $E^{128}G$ and $D^{153}G$ are consistent with inactivation of either of the high affinity EF2 or EF3 due to removal of an essential Ca^{2+} binding side chain. The effect of $F^{149}S$, which suppresses a bond that links EF3 to the W^{129} coelenterazine binding residue (17), presumably results from impairment of EF3 contribution to bioluminescence. The effect of $Q^{168}R$ likely results from interactions of arginine with several Ca^{2+} binding residues of EF3 (17).

These results are consistent with EF1 having a lower affinity to Ca^{2+} than EF2 and 3. Analyses of double EF-hand mutants combining $E^{35}G$, $E^{128}G$ and $D^{153}G$ substitutions (figure

2B) confirmed the differences in EF-hand Ca^{2+} affinities and indicate that a single EF-hand is sufficient to trigger bioluminescence. For these mutants where only one EF-hand was left intact, Ca^{2+} EC50 values were 34 ± 9 µM for $EF1^{+}2^{-}3^{-}$, 6.1 ± 0.1 µM for $EF1^{-}2^{+}3^{-}$ and 7.6 ± 0.6 µM for $EF1^{-}2^{-}3^{+}$. The Ca^{2+} sensitivities of $EF1^{-}2^{+}3^{-}$ or $EF1^{-}2^{-}3^{+}$, lower than that of WT, suggest that mutation of either EF-hand of the EF2-3 pair reduced the affinity of the remaining EF-hand, as reported for other Ca^{2+} binding proteins (8,19). Hence, affinities of WT EF2 and 3 are presumably higher than suggested by the Ca^{2+} sensitivities of $EF1^{-}2^{+}3^{-}$ or $EF1^{-}2^{-}3^{+}$ mutants.

These results indicate that the three EF-hands are endowed with different Ca^{2+} affinities and all contribute to the sensitivity of WT aequorin to $[Ca^{2+}]$.

Luminescence decay kinetics and light integral

Luminescence decays were next analyzed to examine the relationships of the decay rate and light integral with the intensity of the response to Ca^{2+} (figure 3). Decays of WT and mutant aequorins were best fitted with two exponentials (see supporting information). Time constants of these fast and slow exponentials (τ_F and τ_S, respectively) and their light integrals (Σ_F and Σ_S, respectively) were determined and plotted together with total light integral ($\Sigma_T = \Sigma_F + \Sigma_S$) and initial maximum intensity. Since kinetics of SloDK mutants for a given EF-hand (e.g. $E^{35}G$ and $V^{44}A$ for EF1) were similar, only one example is displayed per EF-hand. Kinetics of $Q^{168}R$ and $L^{170}I$ Bright mutants (not shown) were similar to WT, except for a shift towards higher $[Ca^{2+}]$. Similar results were obtained on WT aequorin and the $D^{153}G$ mutant using a fast mixing stopped-flow apparatus (see supporting information).

For WT aequorin, the decay rate increased with $[Ca^{2+}]$ (upper panel) while Σ_T was maximal at low $[Ca^{2+}]$ and remained roughly constant (lower panel). Indeed, correction for the lag preceding the activity measurement (see methods and supporting information) yielded a Σ_T value at 1.24 mM Ca^{2+} which was only decreased to 91.5 % of maximum. Variations of the decay rate thus determined the increase of initial intensity. The curves of initial intensity and Σ_F were almost superimposed, indicating that variations of τ_S contributed little to the increase of the decay rate. Hence, the increase of luminescence intensity was driven primarily by the Σ_F/Σ_T ratio (not shown) which increased from 25.5 ± 2.2 % at 2.7 µM Ca^{2+} to 51.2 ± 0.4 % at 1.24 mM Ca^{2+}.

$N^{26}D$ essentially differed from WT in that Σ_F decreased with increasing $[Ca^{2+}]$ while Σ_S remained roughly constant. As a consequence, $N^{26}D$ exhibited a much smaller increase of decay rate, and thus of initial intensity, than WT. In contrast with WT and Bright mutants, the luminescence decay rates of SloDK mutants decreased with increasing $[Ca^{2+}]$. These

mutants exhibited high τ_S and Σ_S/Σ_T values and extensive variations of Σ_T which determined to a large extent the increase of initial intensity.

The τ_F value varied little with [Ca^{2+}] or between WT and mutants, suggesting it is an intrinsic constant of aequorin luminescence. In WT, τ_F was 615 ± 21 ms at 1.24 mM Ca^{2+}, close to the 833 ms reported assuming monoexponential decay (16). In contrast, other kinetic parameters appeared to depend on EF-hand domains. All SloDK mutations resulted in high τ_S and Σ_S/Σ_T values and altered their variations. Hence, these parameters did not rely on any single EF-hand. Σ_F showed a critical dependence on both EF1 and 3. Indeed, Σ_F/Σ_T was negligible in $E^{35}G$ and $D^{153}G$ (maximum, 1.1 ± 0.4 % and 3.6 ± 1.1 %, respectively). $EF2^-$ SloDK mutants exhibited a markedly different behavior. In these latter mutants, Σ_F persisted throughout the whole [Ca^{2+}] range (maximum Σ_F/Σ_T, 42.8 ± 5.2 % at 12.5 µM Ca^{2+} for $D^{117}G$), while τ_S first decreased (in the range of EF3 affinity) and then increased (in the range of EF1 affinity) with increasing [Ca^{2+}]. This suggests a distinctive role for EF2, perhaps in the functional coupling between EF1 and EF3 domains.

Decays of double EF-hand mutants (not shown) analyzed at saturating [Ca^{2+}] exhibited both a fast and a slow component, confirming these are intrinsic to aequorin luminescence. Values of τ_F were 5.9 ± 0.1 s, 5.5 ± 0.3 s and 8.4 ± 0.5 s and of τ_S were 122 ± 6 s, 275 ± 7 s and 341 ± 28 s for $EF1^+2^-3^-$, $EF1^-2^+3^-$ and $EF1^-2^-3^+$ mutants, respectively. Decays of these mutants were governed by the slow component (Σ_S/Σ_T > 98 %).

The present data suggest that in WT aequorin, all EF-hands contribute to the decay rate increase by modulating the Σ_F/Σ_T ratio, which in turn determines the increase of peak intensity at constant light integral.

Contribution of Q^{168} and L^{170} to decay kinetics

The $QHL^{[168-170]}$ residues interact with both the E^{164} Ca^{2+} binding residue of EF3 and coelenterazine (via the E^{164}-Q^{168} and H^{169}-coelenterazine bonds, see ref. 11), and may help triggering bioluminescence (17). This provides a rationale for the lower Ca^{2+} sensitivity of $Q^{168}R$ and $L^{170}I$ mutants, and suggests that these residues contribute to decay kinetics. Indeed, screening of a library of random Q^{168} and L^{170} mutants resulted in the isolation of mutants exhibiting a large range of decay rates (see supporting information). Among selected clones, the $Q^{168}A\&L^{170}V$ mutant (designated AHV) and the mutant combining $Q^{168}R$ and $L^{170}I$ Bright mutations (designated RHI) were characterized in detail. Indeed, their Ca^{2+} sensitivities were reduced to a similar extent (EC50 values: 28 ± 2 and 16.5 ± 0.6 µM for AHV and RHI, respectively), but their decay rates differed markedly (figure 4).

RHI bioluminescence exhibited all the key features of WT, but shifted towards higher [Ca^{2+}]. This shift allowed the initial increases of Σ_F, Σ_S and Σ_T, which occurred below 2.7 µM

Ca^{2+} for WT, to be observed above this concentration for RHI. In this initial phase, Σ_S and Σ_T increased in parallel and reached a maximum at 12.5 µM Ca^{2+}. Beyond this point, Σ_T remained close to its maximum (corrected Σ_T for lag between injection and measurement, 84.2 % at 1.24 mM Ca^{2+}) while kinetics varied extensively. As for WT, most of the increase of RHI initial intensity with [Ca^{2+}] resulted from an increase of Σ_F. Hence, RHI mutations reduced EF3 Ca^{2+} affinity but left the transduction of Ca^{2+} induced conformational changes to bioluminescence unaffected.

In contrast, the slow decay kinetics of AHV suggests that the contribution of EF3 to the response to Ca^{2+} was reduced in this mutant. Indeed, AHV kinetics exhibited high τ_S and Σ_S/Σ_T values and Σ_T variations extending over a large [Ca^{2+}] range, as found in $EF3^-$ SloDK mutants. This presumably resulted in part from the disruption of E^{164}-Q^{168} interaction. However, the decrease of τ_S and the persistence of Σ_F throughout the whole [Ca^{2+}] range (Σ_F/Σ_T, 2.5 ± 0.7 % at 1.24 mM Ca^{2+}) suggests that, in contrast with $EF3^-$ SloDK mutants, the participation of EF3 to bioluminescence was not abolished in the AHV mutant.

These data confirm that slow decay kinetics result from the disruption of a link between a given EF-hand domain and coelenterazine binding residues, but not from the reduction of its calcium affinity.

A model of aequorin Ca^{2+} dependence

The present results suggest that the three EF-hands contribute to luminescence and that varying proportions of a slow and a fast light emitting state (S-Aeq and F-Aeq, respectively) determine the increase of the decay rate and thus of light intensity. This is summarized in figure 5A, which postulates that EF1 has lower Ca^{2+} affinity than EF2 and 3. This scheme does not infer sequential Ca^{2+} binding to the different EF-hands but describes their occupancy with increasing [Ca^{2+}].

None of the reaction schemes and models of aequorin luminescence proposed so far (16,20) takes into account the variations of decay rate with [Ca^{2+}] as a key determinant of light intensity. Hence, we investigated whether a model based on these variations may capture the essential features of aequorin responses to Ca^{2+} (figure 5B, see equations in supporting information). This model postulates a) an equilibrium between S-Aeq and F-Aeq whose interconversion constant (K_{SF}) depends on the number of Ca^{2+} bound, b) Σ_F/Σ_T and Σ_S/Σ_T vary with the binding of *n* Ca^{2+} to an initial Ca^{2+} bound specie (S-AeqCa_i), c) τ_F is independent of [Ca^{2+}] (set at mean experimental value) and τ_S varies with the binding of Ca^{2+} to *m* sites, and d) light emission efficiency Σ_T ($\Sigma_F+\Sigma_S$) is constant for all Ca^{2+} bound species.

Parameters of the equation describing theoretical τ_S were optimized to fit experimental τ_S values measured for WT aequorin (see supporting information). The best fit (see curve on

figure 5C) was obtained with *m*=1.5 Ca^{2+}, binding with an apparent dissociation constant of 3.8 µM. Hence, acceleration of τ_S in WT aequorin requires binding of more than one Ca^{2+} in our model. Similar optimization was performed for theoretical Σ_S/Σ_T. The best fit (see Σ_S/Σ_T and Σ_F/Σ_T curves on figure 5C) was obtained with K_{SF1}=0.3, K_{SF2}=1, and *n*=1.9 Ca^{2+} binding with an apparent dissociation constant of 17 µM. These values imply that in our model, the proportion of molecules in the F state increases (because of $K_{SF2} > K_{SF1}$) as a result of the binding of more than one Ca^{2+}. Since aequorin contains only three EF-hands, the *m* and *n* values derived from the best fit predict that at least one EF-hand is involved in both τ_S and Σ_F/Σ_T variations, consistent with their overlapping [Ca^{2+}] ranges. Our model predicts that SloDK mutations have a major effect on K_{SF} interconversion constants. While $EF1^-$ and $EF3^-$ mutations would decrease both K_{SF1} and K_{SF2}, $EF2^-$ mutations would leave K_{SF1} relatively unaffected.

Finally, evolution of the theoretical initial intensity with [Ca^{2+}] was calculated from Σ_S/Σ_T, Σ_F/Σ_T and τ_S values derived from the best fit, with constant τ_F (see supporting information). The good match observed between theoretical and experimental values (figure 5C, right), indicates that the present model of WT aequorin adequately describes the parallel increases of light intensity and decay rate with [Ca^{2+}] occurring at constant light integral.

DISCUSSION

The contribution of aequorin EF-hand domains to bioluminescence was dissected using mutants of decay kinetics and Ca^{2+} sensitivity. All EF-hand domains contributed to Ca^{2+} sensitivity with EF1 showing lower affinity than EF2 and 3, and each individual EF-hand was able to trigger luminescence. Decay kinetics of WT aequorin consisted of a slow and a fast component whose variations determined those of luminescence intensity in a large [Ca^{2+}] range where light integral was constant. All EF-hand domains contributed to these variations. These findings were used to design a model that adequately described the Ca^{2+} dependence of WT aequorin.

SloDK mutations impair transduction of Ca^{2+} binding to bioluminescence

In EF-hand based Ca^{2+} sensors like aequorin and calmodulin, Ca^{2+} binding induces conformational changes that trigger activity (8). While Bright mutations essentially shifted Ca^{2+} sensitivity curves, SloDK ones additionally decreased the rate of light emission, presumably by disrupting a structural link which allows a given EF-hand to trigger luminescence. Indeed, D/E to G substitutions at EF1-3 extremities likely uncouple the EF-hand from the protein scaffold by increasing the flexibility of its joint to the adjacent α-helix. The $V^{44}A$ and $F^{149}S$ mutations do not affect Ca^{2+} binding residues, and may thus specifically impair conformational changes. Such a case has been reported for calmodulin where the EF3 neighboring mutation $F^{92}A$ impairs conformational changes without reducing Ca^{2+} affinity (21). The $F^{149}S$ mutation suppresses a link of EF3 to the W^{129} coelenterazine binding residue (17). Moreover, the $V^{44}A$ mutation may affect the interaction of V^{44} with the A^{40} coelenterazine binding residue (11). Interestingly, corresponding residues of the photoprotein obelin both interact with coelenterazine (A^{46} and I^{50}, see supporting information and ref. 22). Finally, RHI and AHV mutants provide an example of mutations at the same positions which resulted in similar Ca^{2+} EC50s but very different decay rates. Part of this difference can be attributed to disruption of the E^{164}-Q^{168} bond that links EF3 conformational changes to bioluminescence (17). It thus appears that SloDK mutants all disrupt a structural link that allows Ca^{2+} binding to trigger bioluminescence.

Functional domains of aequorin

The structures of photoproteins suggest that each of the three EF-hand domains forms a functional unit (11, 22). Indeed, results with double EF-hand mutants indicate that each individual EF-hand is able to trigger aequorin bioluminescence. Nonetheless, distinctive functional properties could be assigned to each of the three EF-hand domains, based on the

different effects of their respective mutations. These differences appear very significant, given the high similarity between effects of the two SloDK mutations found for each EF-hand. Our results define a low Ca^{2+} affinity EF1 domain and a high affinity domain comprising the EF2,3 pair, consistent with a previous report showing that aequorin binds two Ca^{2+} with a high affinity and an additional Ca^{2+} with 22 times lower affinity (23). The N and C-terminal domains of calmodulin similarly exhibit low and high Ca^{2+} affinity, respectively (19). Interestingly, the cooperativity between aequorin EF2,3 for Ca^{2+} binding, suggested by the low affinity of $EF1^{-}2^{+}3^{-}$ or $EF1^{-}2^{-}3^{+}$ mutants as compared to WT, is also observed for the C-terminal EF-hand pair of calmodulin (19). Finally, $[Ca^{2+}]$ dependence of kinetic properties relied heavily on EF1 and EF3, but less on EF2 (see Σ_F and τ_S in $EF2^{-}$ mutants) which may be preferentially involved in the coupling between the low affinity EF1 and the high affinity EF3. Previous studies reported that aequorin bioluminescence involves the binding of two or more Ca^{2+} (20,23). Our results indicate that although each individual EF-hand is sufficient to trigger luminescence, all three EF-hands participate in the dependence of WT aequorin luminescence on $[Ca^{2+}]$.

Decay kinetics, light integral and initial maximum intensity

Our data show that in WT aequorin, both the light intensity and the decay rate are greater at higher $[Ca^{2+}]$, such that the total light (integral, Σ_T) is the same at different Ca^{2+} concentrations. Although the $[Ca^{2+}]$ dependence of the decay rate has been early reported (16), the present study reveals that this results from variations of a fast and a slow component. The fast and slow components co-existed across mutants and Ca^{2+} concentrations and were even observed in double EF-hand mutants where only one EF-hand is left unaffected. Our results thus suggest that the slow and fast light emitting states co-exist and that their proportions evolve concomitantly, rather than sequentially along a single linear pathway. In any sequential model, τ_F and τ_S would evolve in the same $[Ca^{2+}]$ range as Σ_F/Σ_T and Σ_S/Σ_T, which is in contradiction with our observations. In contrast, our parallel model allows dissociating variations of the different kinetic parameters and adequately describes variations of light intensity with $[Ca^{2+}]$.

A key feature of WT aequorin is that Σ_T reached a maximum at low $[Ca^{2+}]$ and remained roughly constant in a wide $[Ca^{2+}]$ range where major variations of decay kinetics occurred. Given the existence of only three EF-hands in aequorin (6,7,13), this suggests that Σ_T variations rely primarily on the binding of only one Ca^{2+}, as postulated in the present model, while the three EF-hands are involved in variations of decay rate, and thus of peak intensity. It is likely that light emission rate resulting from single EF-hand occupancy is higher in WT

aequorin, where the rigidity of the photoprotein scaffold is unaffected, than in double EF-hand mutants.

Aequorin luminescence as a biological signal

The fast kinetics of photoprotein luminescence provides a sensitive means of studying the early steps, which lead from calcium binding to activation of EF-hand based calcium sensors. The structural homology among various photoproteins suggests that their [Ca^{2+}] dependence obeys the same rules, despite different maximum luminescence rates (24,25). Photoproteins contain a pseudo EF-hand motif, which does not bind Ca^{2+} (6,13). Its position relative to the three EF-hands in the primary sequence, which defines a pattern similar to the two EF-hand pairs of calmodulin, has suggested that photoproteins have evolved from a calmodulin ancestor gene towards bioluminescence (26). As underlined above, some of the present findings may apply to calmodulin and other Ca^{2+} sensors that rely on several EF-hands exhibiting different affinities to transduce Ca^{2+} stimuli into biological signals.

Aequorin occurs in the jellyfish *Aequorea* where it forms a readily mobilizable source of light used to generate a rapid luminescent signal in response to Ca^{2+} transients. In contrast with typical enzymatic systems where the substrate is only metabolized upon activation, aequorin is a reaction intermediate where the coelenterazine substrate is already consumed. Our results indicate that the Ca^{2+} dependence of aequorin luminescence relies on variations of the light emission rate occurring at constant maximal photon yield. Variations of the light emission rate allow the intensity of the light signal to reflect the amplitude of Ca^{2+} transients. It is noteworthy that the steadiness of the photon yield allows aequorin consumption to be proportional to the amplitude of a transient light signal. If alternatively, variations of the photon yield were responsible for variations of light intensity, this would imply non-radiative energy dissipation in case of sub-maximal luminescence response. The mechanisms of aequorin Ca^{2+} dependence thus appear well adapted to the function of signal emitter in the jellyfish, which depends on its diet as an exclusive source of coelenterazine (27).

Acknowledgements: We thank J. Woodland Hastings, Alain-François Chaffotte and Stephen Rees for their valuable help. L.T. was supported by a Fondation pour la Recherche Médicale fellowship.

REFERENCES

1. Shimomura, O., Johnson, F.H. & Saiga, Y. (1962) *J. Cell. Comp. Physiol.* **59**, 223-239
2. Shimomura, O. & Johnson, F.H. (1975) *Nature* **256**, 236-238
3. Shimomura, O. & Johnson, F.H. (1978) *Proc. Natl. Acad. Sci. U S A* **75**, 2611-2615
4. Hastings, J.W. & Gibson, Q.H. (1963) J. Biol. Chem. **238**, 2537-54
5. Wilson, T. & Hastings, J.W. (1998) Annu. Rev. Cell Dev. Biol. **14**, 197-230
6. Inouye, S., Noguchi, M., Sakaki, Y., Takagi, Y., Miyata, T., Iwanaga, S., Miyata, T. & Tsuji, F. I. (1985) *Proc. Natl. Acad. Sci. U. S. A* **82**, 3154-3158
7. Prasher, D., McCann, R. O. & Cormier, M. J. (1985) *Biochem. Biophys. Res. Commun.* **126**, 1259-1268
8. Lewit-Bentley, A. & Rety, S. (2000) *Curr. Opin. Struct. Biol.* **10**, 637-643
9. Tsuji, F. I., Inouye, S., Goto, T. & Sakaki, Y. (1986) *PNAS* **83**, 8107-8111
10. Kendall, J. M., Sala-Newby, G., Ghalaut, V., Dormer, R. L. & Campbell, A. K. (1992) *Biochem. Biophys. Res. Commun.* **187**, 1091-1097
11. Head, J. F., Inouye, S., Teranishi, K. & Shimomura, O. (2000) *Nature* **405**, 372-376
12. Toma, S., Chong, K. T., Nakagawa, A., Teranishi, K., Inouye, S., & Shimomura, O. (2005) *Protein Sci.* **14**, 409-416
13. Deng, L., Vysotski, E.S., Markova, S.V., Liu, Z.J., Lee, J., Rose, J., & Wang, B.C. (2005) *Protein Sci.* **14,** 663-675
14. Brini, M., Pinton, P., Pozzan, T. & Rizzuto, R. (1999) *Microsc. Res. Tech.* **46**, 380-389
15. Shimomura, O., & Johnson, F. H. (1975) *Nature* **256**, 236-238
16. Hastings, J. W., Mitchell, G., Mattingly, P. H., Blinks, J. R. & Van Leeuwen, M. (1969) *Nature* **222**, 1047-1050
17. Tsuzuki, K., Tricoire, L., Courjean, O., Gibelin, N., Rossier, J. & Lambolez, B. (2005) *J. Biol. Chem.* **280**, 34324-34331
18. Bers, D. M., Patton, C. W. & Nuccitelli, R. (1994) *Methods Cell Biol.* **40**, 3-29
19. Maune, J. F., Klee, C. B. & Beckingham, K. (1992) *J. Biol. Chem.* **267**, 5286-5295
20. Allen, D. G., Blinks, J. R. & Prendergast, F. G. (1977) *Science* **195**, 996-998
21. Meyer, D.F., Mabuchi, Y. & Grabarek, Z. (1996) *J. Biol. Chem*. **271**, 11284-11290
22. Liu, Z.J., Vysotski, E.S., Chen, C.J., Rose, J.P., Lee, J. & Wang, B.C. (2000) *Protein Sci.* **9,** 2085-2093
23. Shimomura, O. (1995) *Biochem. Biophys. Res. Commun.* **211**, 359-363
24. Morin, J.G. & Hastings, J.W. (1971) *J Cell Physiol*. **77**, 305-312
25. Markova, S. V., Vysotski, E. S., Blinks, J. R., Burakova, L. P., Wang, B. C., & Lee, J. (2002) *Biochemistry* **41,** 2227-2236
26. Tsuji, F.I., Ohmiya, Y., Fagan, T.F., Toh, H. & Inouye, S. (1995) *Photochem. Photobiol*. **62**, 657-661
27. Haddock, S. H., Rivers, T. J., & Robison, B. H. (2001) *Proc.Natl.Acad.Sci.U.S.A* **98**, 11148-11151

FIGURE LEGENDS

Figure 1

Bright and SloDK aequorin mutants. **A**. Bright (above) and SloDK (below) mutations of apoaequorin were located inside EF-hands (boxes) or nearby. **B**. Times to reach half of initial light ($t_{1/2}$) obtained at saturating [Ca^{2+}] for WT and mutant aequorins reflect luminescence decay kinetics. Ca^{2+} EC50 values derived from curves of [Ca^{2+}]-dependent luminescence intensities.

Figure 2

Initial maximum intensity against [Ca^{2+}] of mutant and WT aequorins. **A**. Bright and SloDK mutants. The plot of the $L^{170}I$ Bright mutant (not shown) was almost identical to that of $Q^{168}R$. **B**. Double EF-hand mutants. $EF1^{+}2^{-}3^{-}$, $EF1^{-}2^{+}3^{-}$ and $EF1^{-}2^{-}3^{+}$ correspond to the $E^{128}G\&D^{153}G$, $E^{35}G\&D^{153}G$ and $E^{35}G\&D^{128}G$ double mutants, respectively.

Figure 3

Decay kinetics of WT aequorin and EF-hand mutants. ***Upper***: unitary recordings show variations of decay kinetics between low (dotted gray), medium low (gray), medium high (dotted black) and high (black) [Ca^{2+}]. ***Middle***: plots of the time constants of fast (τ_F) and slow (τ_S) exponentials versus [Ca^{2+}] (x-axis as in lower panels). In $E^{35}G$ and $D^{153}G$, τ_F values could not be determined above 12.5 µM Ca^{2+} due to breakdown of Σ_F. ***Lower***: Light integrals of the fast (Σ_F) and slow (Σ_S) exponentials and of total light emitted ($\Sigma_T = \Sigma_F + \Sigma_S$) versus [$Ca^{2+}$]. Initial intensities are plotted for comparison.

Figure 4

Decay kinetics of Q^{168} and L^{170} double mutants. RHI: $Q^{168}R$ & $L^{170}I$, AHV: $Q^{168}A$ & $L^{170}V$. ***Upper***: unitary recordings show decay kinetics at low (dotted gray), medium low (gray), medium high (dotted black) and high (black) [Ca^{2+}]. ***Middle***: Time constants of fast (τ_F) and slow (τ_S) exponentials versus [Ca^{2+}] (x-axis as in lower panels). ***Lower***: Light integrals of the fast (Σ_F) and slow (Σ_S) exponentials, of total light emitted ($\Sigma_T = \Sigma_F + \Sigma_S$) and of initial intensity versus [Ca^{2+}].

Figure 5

A model of WT aequorin Ca^{2+} dependence. **A.** Ca^{2+} binding pathways and interconversion between a slow (S) and a fast (F) light emitting state. Ca^{2+} bound EF-hands are shown in gray. **B.** ***Upper***: interconversion equilibria describing evolution of S and F state proportions with Ca^{2+} binding. ***Lower***: kinetics of light emission from Ca^{2+} bound S and F states. **C.** Comparison of experimental values of kinetic parameters (symbols) with the best fit of the model (curves).

Figure 1

A

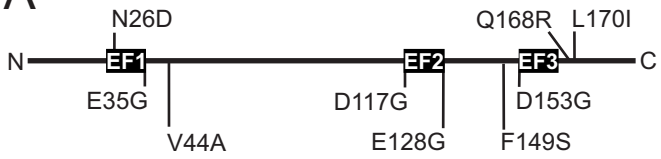

B

Mutation	Pos.	Type	$t_{1/2}$ (s)	Ca^{2+} EC_{50} (μM)
WT	-	-	0.7 ± 0.01	2.6 ± 0.3
N26D	EF1	Bright	1.1 ± 0.02	< 2.6
E35G	EF1	SloDK	39.9 ± 1.5	< 2.6
V44A	EF1	SloDK	33.7 ± 0.8	< 2.6
D117G	EF2	SloDK	28.6 ± 1.3	109 ± 20
E128G	EF2	SloDK	17.0 ± 0.6	23 ± 2
F149S	EF3	SloDK	13.7 ± 0.6	61 ± 3
D153G	EF3	SloDK	27.8 ± 0.5	49 ± 4
Q168R	EF3	Bright	0.7 ± 0.003	6.8 ± 0.1
L170I	EF3	Bright	1.6 ± 0.002	9.1 ± 0.1

Figure 2

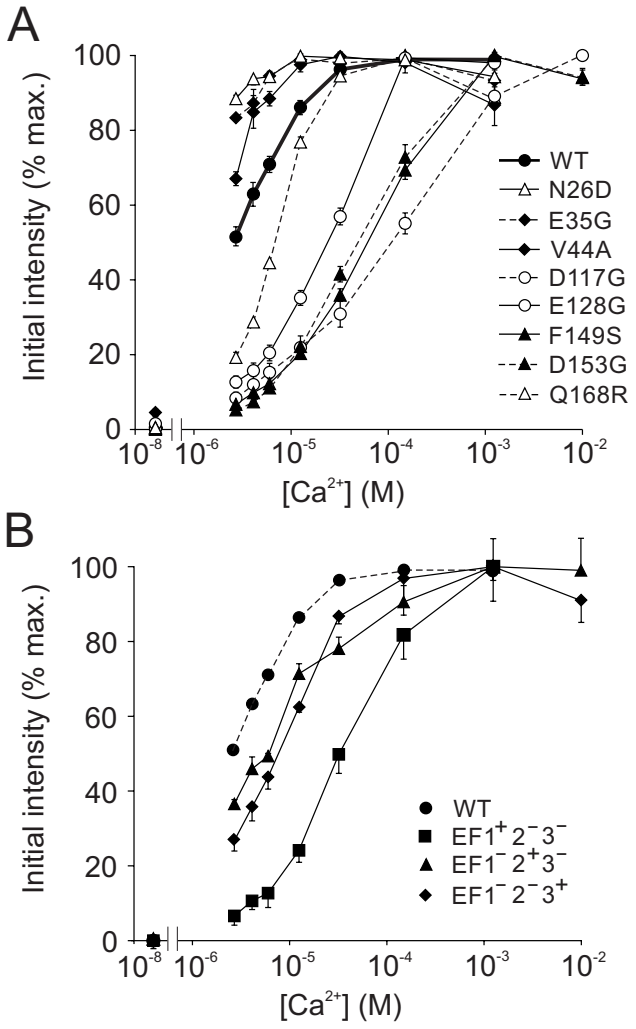
A
Initial intensity (% max.)
100
80
60
40
20
0
WT
N26D
E35G
V44A
D117G
E128G
F149S
D153G
Q168R
10-8 10-6 10-5 10-4 10-3 10-2
[Ca2+] (M)
B
Initial intensity (% max.)
100
80
60
40
20
0
WT
EF1+2-3-
EF1-2+3-
EF1-2-3+
10-8 10-6 10-5 10-4 10-3 10-2
[Ca2+] (M)

Figure 3

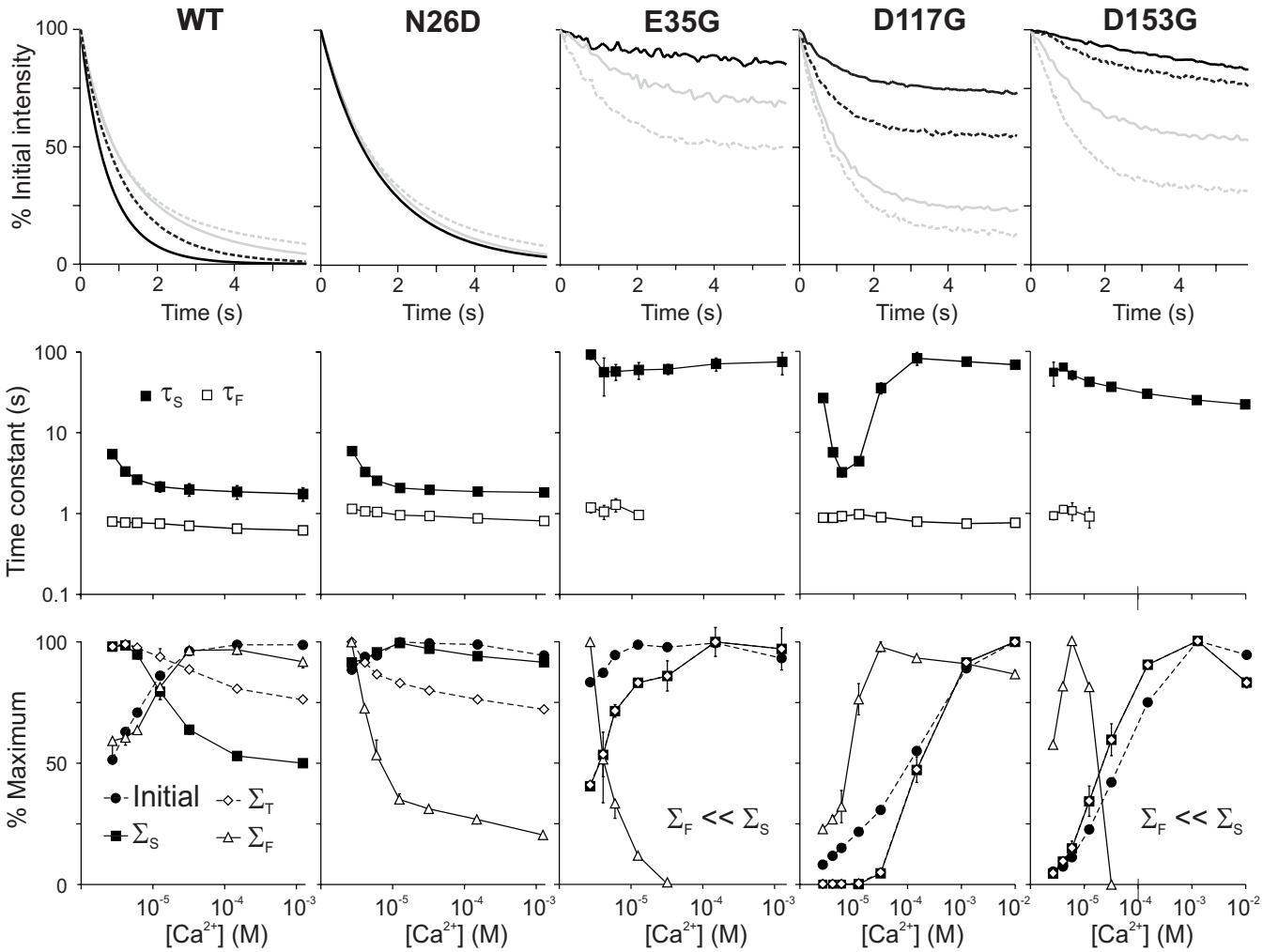
WT
N26D
E35G
D117G
D153G
% Initial intensity
Time (s)
Time constant (s)
τS τF
% Maximum
Initial
ΣT
ΣS
ΣF
ΣF << ΣS
[Ca2+] (M)

Figure 4

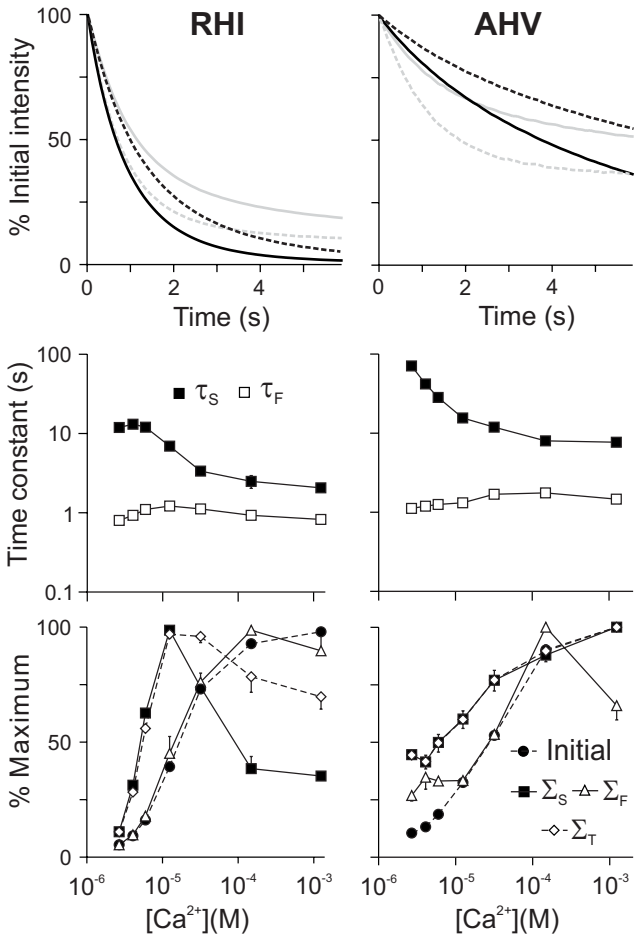
RHI
AHV
% Initial intensity
100
50
0
0
2
4
Time (s)
Time constant (s)
100
10
1
0.1
τ_S
τ_F
% Maximum
100
50
0
10^{-6}
10^{-5}
10^{-4}
10^{-3}
$[Ca^{2+}](M)$
Initial
Σ_S
Σ_F
Σ_T

Figure 5

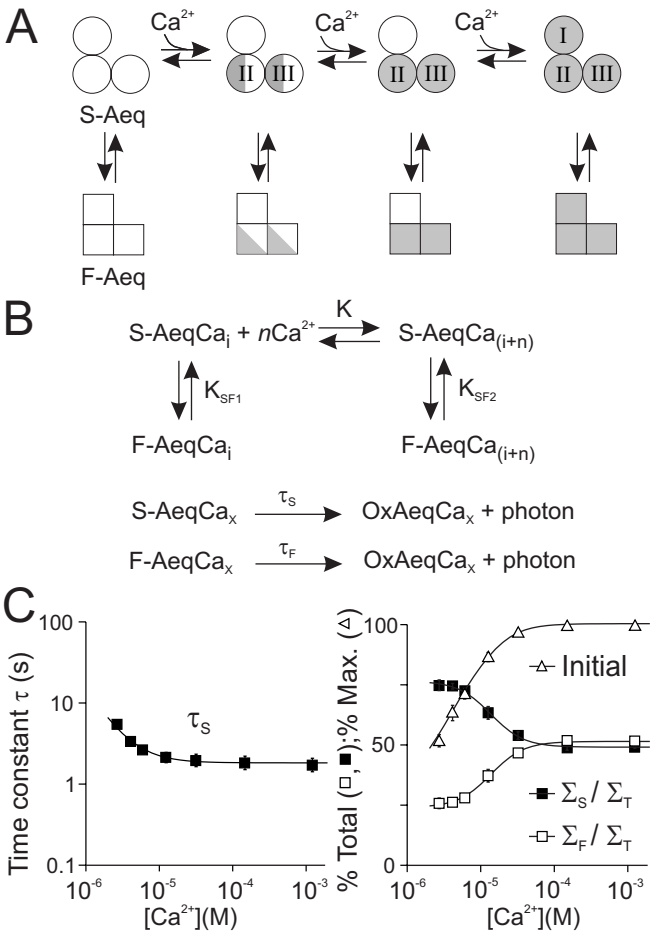
A
Ca2+
Ca2+
Ca2+
I
II
III
II
III
II
III
S-Aeq
F-Aeq
B
S-AeqCa_i + nCa2+
K
S-AeqCa_(i+n)
K_SF1
K_SF2
F-AeqCa_i
F-AeqCa_(i+n)
S-AeqCa_x
τ_S
OxAeqCa_x + photon
F-AeqCa_x
τ_F
OxAeqCa_x + photon
C
Time constant τ (s)
100
10
1
0.1
τ_S
10-6
10-5
10-4
10-3
[Ca2+](M)
% Total (□,■);% Max. (△)
100
50
0
Initial
Σ_S / Σ_T
Σ_F / Σ_T
10-6
10-5
10-4
10-3
[Ca2+](M)

SUPPORTING INFORMATION

This supplement contains:

- Supporting Methods
- Supporting Results
- Supporting References
- Supporting Figure Legends
- Supporting Figures

SUPPORTING MATERIALS AND METHODS

Luminescence assays using a fast mixing stopped-flow apparatus

WT and mutant aequorins were reconstituted as described in main text (EDTA, 10 µM) and diluted in a decalcified Tris (pH8), 50mM solution (final EDTA, 0.6 µM). Decalcified Tris solutions were prepared with a column packed with chelex-100 resin (Biorad, Hercules, CA) according to manufacturer's instructions. Decay kinetics of bioluminescence were recorded in a SF 300 stopped-flow device (Biologic, Grenoble, France) equipped with a photomultiplier. Light emission was initiated in the stopped-flow apparatus by mixing 60 µl of the photoprotein solution with 140 µl of a Tris (pH8), 50mM solution containing variable $CaCl_2$ concentrations. Data were acquired at 100 Hz. Each value represents the mean of two experiments with at least four shots per [Ca^{2+}]. Results are expressed as mean ± SEM. Complete data is available by e-mail on request.

A model of aequorin calcium sensitivity

Following equations describe reaction schemes in figure 5B (main text) and derive from Hill and MWC formalisms (1,2). Experimental ratios of Σ_S/Σ_T were fitted to the following theoretical expression using the Origin 5.0 software (Microcal, Northampton, MA, USA).

$$\Sigma_S / \Sigma_T = \frac{K^n + \left[Ca^{2+}\right]^n}{K^n\left(1 + K_{SF1}\right) + \left(1 + K_{SF2}\right)\left[Ca^{2+}\right]^n}$$

K is the apparent dissociation constant of Ca^{2+} binding, n is the corresponding Hill coefficient, and K_{SF1} and K_{SF2} are interconversion constants between the slow (S) and fast (F) emitting forms at low (K_{SF1}) and high (K_{SF2}) [Ca^{2+}]. These equilibrium constants are defined by the following equations:

$$K^n = \frac{[SAeqCa_i][Ca]^n}{[SAeqCa_{(i+n)}]}\ ;\ K_{SF1} = \frac{[FAeqCa_i]}{[SAeqCa_i]}\ ;\ K_{SF2} = \frac{[FAeqCa_{(i+n)}]}{[SAeqCa_{(i+n)}]}$$

Experimental τ_s values were fitted to:

$$\tau_S = \tau_0 \frac{K_0^m + \left[Ca^{2+}\right]^m}{\left[Ca^{2+}\right]^m}$$

where K_0 is the apparent dissociation constant of Ca^{2+} binding, m is the corresponding Hill coefficient, and τ_0 is the time constant at saturating $[Ca^{2+}]$.

Determination of theoretical initial maximum intensity

Theoretical initial amplitudes of the fast and slow components were calculated from Σ_S/Σ_T, Σ_F/Σ_T, τ_F and τ_S values derived from the best fit of the model with experimental data, according to equations:

$$I_{fast} = \frac{\Sigma_F / \Sigma_T}{\tau_F} \quad \text{and} \quad I_{slow} = \frac{\Sigma_S / \Sigma_T}{\tau_S}$$

Theoretical initial activity (I) was calculated from corrected initial amplitudes (I^*_{fast} and I^*_{slow}) to take into account the lag of 365 ms between the beginning of Ca^{2+} injection and activity measurement in our experimental setup, according to equation:

$$I = I^*_{fast} + I^*_{slow} = I_{fast}\ e^{-\frac{0.365}{\tau_S}} + I_{slow}\ e^{-\frac{0.365}{\tau_F}}$$

SUPPORTING RESULTS

Screening random Q^{168} and L^{170} aequorin mutants for decay kinetics

Construction of a library of random Q^{168} and L^{170} mutants and expression in E. coli has been described in a previous report (3). Bioluminescence was analyzed in a luminometer by applying a Ca^{2+}-triton solution onto intact bacteria (3). Analysis of 500 clones showed that the mean bioluminescence intensity was reduced to 5.2 % of WT, indicating that most Q^{168} or L^{170} substitutions disrupt aequorin function, consistently with a direct role of $QHL^{[168-170]}$ residues in bioluminescence. Subsequently, 3840 clones were screened for both resistance to a 30 min heat shock at 55°C and for decay kinetics of light emission. Characterization of thermostability of the mutants has been previously reported (3). The light emitted during the first 2 seconds after injection (L_{0-2}) and during the 2 following seconds (L_{2-4}) was measured. As aequorin flash bioluminescence follows an exponential decay, the L_{2-4}/L_{0-4} ratio is an index of decay kinetics. Among 191 heat resistant clones, 29 were selected for sequence analysis that showed a range of kinetics (supporting figure 3, left) similar to that of the population of 191 clones. Mutants at the $QHL^{[168-170]}$ triplet are designated by aminoacid sequence (e.g. the AHV is the double Q^{168}A & L^{170}V mutant). Amino acids found at position 168 were R, S, K or A and were I, V, F M or L at position 170. Only hydrophobic residues were detected at position 170. Both positions influenced kinetics with, from slow to fast: A, K, R at position 168 and I, V, F, L at position 170 (supporting figure 3, right). The fast RHL mutant corresponds to the Bright Q^{168}R whose decay kinetics were similar to WT aequorin. Characterizations of the AHV mutant that presented slowest decay kinetics and of the RHI mutant whose kinetics were intermediate between AHV and RHL are described in main text.

SUPPORTING REFERENCES

1. Hill, A. V. (1910) *J. Physiol. Lond.* **40**, 4-7

2. Monod, J., Wyman, J. & Changeux, J. P. (1965) *J. Mol. Biol.* **12:88-118.**, 88-118

3. Tsuzuki, K., Tricoire, L., Courjean, O., Gibelin, N., Rossier, J. & Lambolez, B. (2005) *J. Biol. Chem.* **280**, 34324-34331

4. Illarionov, B. A., Bondar, V. S., Illarionova, V. A. & Vysotski, E. S. (1995) *Gene* **153**, 273-274

5. Inouye, S. & Tsuji, F. I. (1993) *FEBS Lett.* **315**, 343-346

6. Fagan, T. F., Ohmiya, Y., Blinks, J. R., Inouye, S. & Tsuji, F. I. (1993) *FEBS Lett.* **333**, 301-305

7. Head, J. F., Inouye, S., Teranishi, K. & Shimomura, O. (2000) *Nature* **405**, 372-376

8. Liu, Z.J., Vysotski, E.S., Chen, C.J., Rose, J.P., Lee, J. & Wang, B.C. (2000) *Protein Sci.* **9,** 2085-2093

SUPPORTING FIGURE LEGENDS

Supporting Figure 1

Multiple alignment of aequorin, obelin (4), clytin (5) and mitrocomin (6) primary sequences. Gray boxes indicate EF hands. Blue boxes denote aminoacid residues forming the coelenterazine binding pocket, as reported from the crystal structure of WT aequorin (7) and obelin (8). Twenty-one out of 23 coelenterazine binding residues belong to α-helices adjacent to EFs (7,8). Orange boxes show positions of Bright and SloDK mutations and conserved residues at corresponding positions in other photoproteins.

Supporting Figure 2

Analysis of decay kinetics. **A.** Logarithmic plots of WT and mutant aequorins bioluminescence decays shown in figure 3, main text. For WT and $N^{26}D$, the arrows indicate the slope of luminescence decay at the beginning of the recording of their response to high [Ca^{2+}]. Note that decays were not linear and thus cannot be described by a single exponential. **B.** Comparison of luminescence decay of WT aequorin and SloDK $D^{117}G$ mutant (colored lines) with results of fit by two decaying exponentials (dotted lines). WT and mutant aequorin decay kinetics were best fitted with the sum of two decaying exponentials according to the formula $[I_S \exp(-t/\tau_S)+I_F \exp(-t/\tau_F)]$, where I_S and I_F represent their intensities at t=0, and τ_S and τ_F represent their time constants. The light integrals corresponding to these exponentials (Σ_S and Σ_F) were calculated from the products $I_S.\tau_S$ and $I_F.\tau_F$.

Supporting Figure 3

Decay kinetics of WT aequorin luminescence obtained with a fast mixing stopped-flow apparatus. **A.** Responses to low (red), medium (green) and high (black) [Ca^{2+}]. **B.** Logarithmic plots of luminescence decays shown in A. The arrows indicate the slope of luminescence decays 100ms after the peak. Note that decays were not linear and thus cannot be described by a single exponential. **C.** Plots of the time constants of slow (τ_S) and fast (τ_F) exponentials versus [Ca^{2+}]. **D.** Plots of maximum peak intensity, light integrals of the fast (Σ_F) and slow (Σ_S) exponentials and of total light emitted ($\Sigma_T = \Sigma_F + \Sigma_S$) versus [$Ca^{2+}$]. **E.** Plots of the contribution of the slow and fast components of luminescence decay to the total light integral (Σ_S/Σ_T and Σ_F/Σ_T respectively).

Supporting Figure 4

Decay kinetics of $D^{153}G$ aequorin mutant luminescence obtained with a fast mixing stopped-flow apparatus. **A.** Responses to low (red), medium (green) and high (black) [Ca^{2+}]. **B.** Logarithmic plots of luminescence decays shown in A. The arrows indicate the slope of luminescence decays 100ms after the peak. Note that decays were not linear and thus cannot be described by a single exponential. **C.** Plots of the time constants of slow (τ_S) and fast (τ_F) exponentials versus [Ca^{2+}]. **D.** Plots of maximum peak intensity, light integrals of the fast (Σ_F) and slow (Σ_S) exponentials and of total light emitted ($\Sigma_T = \Sigma_F + \Sigma_S$) versus [$Ca^{2+}$]. **E.** Plots of the contribution of the slow and fast components of luminescence decay to the total light integral (Σ_S/Σ_T and Σ_F/Σ_T respectively).

Supporting Figure 5

Left panel: Bioluminescence decay rates ($L_{2\text{-}4}/L_{0\text{-}2}$) of bacterial clones expressing Q^{168} and L^{170} aequorin mutants. These mutants are designated by their aminoacid sequence at the $QHL^{[168\text{-}170]}$ triplet (e.g. the AHV is the double $Q^{168}A$ & $L^{170}V$ mutant). High $L_{2\text{-}4}/L_{0\text{-}2}$ values denote slow decay kinetics. ***Right panel*** shows the influence of various aminoacid substitutions at positions 168 and 170 on decay rate.

Supporting figure 1

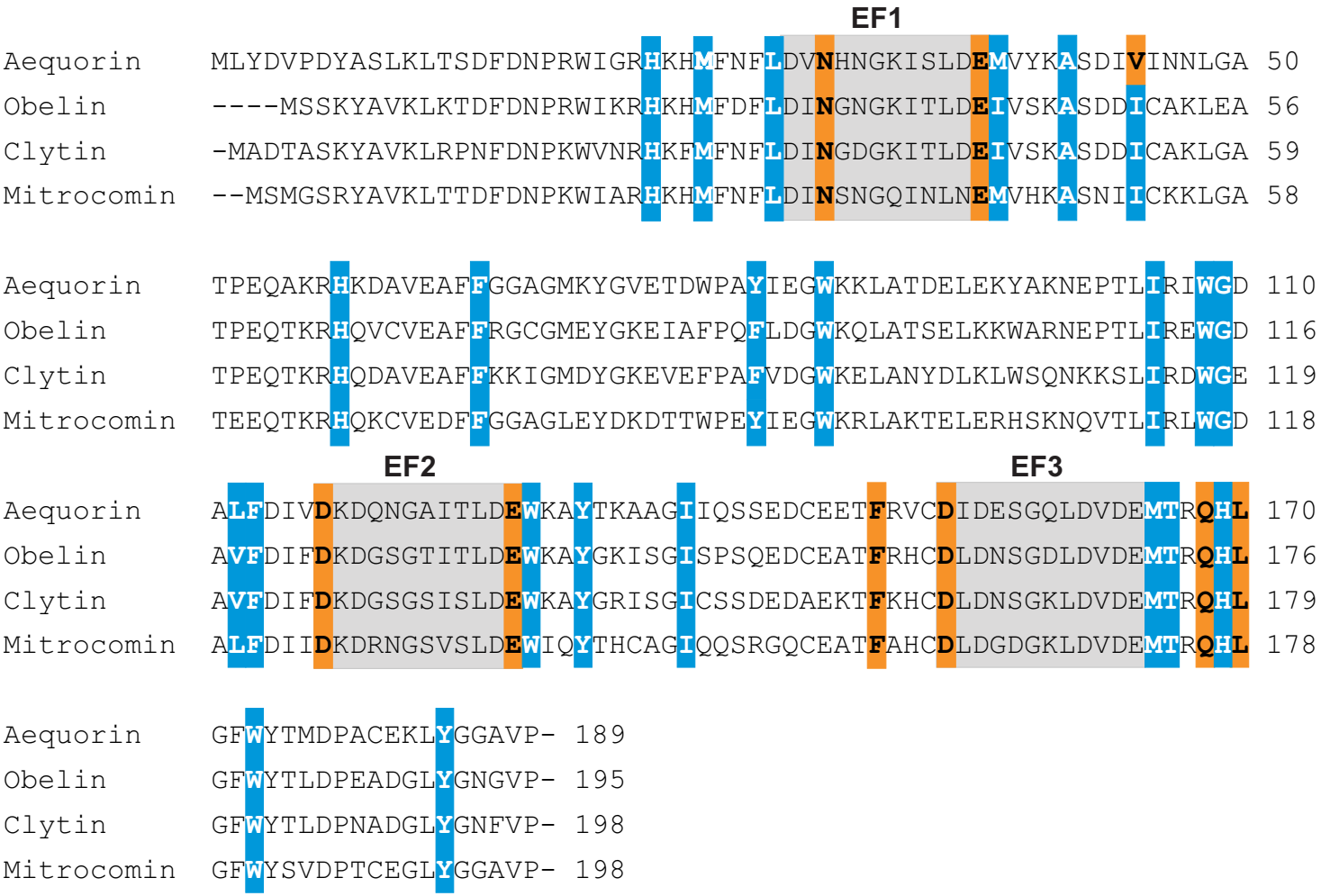

Supporting figure 2

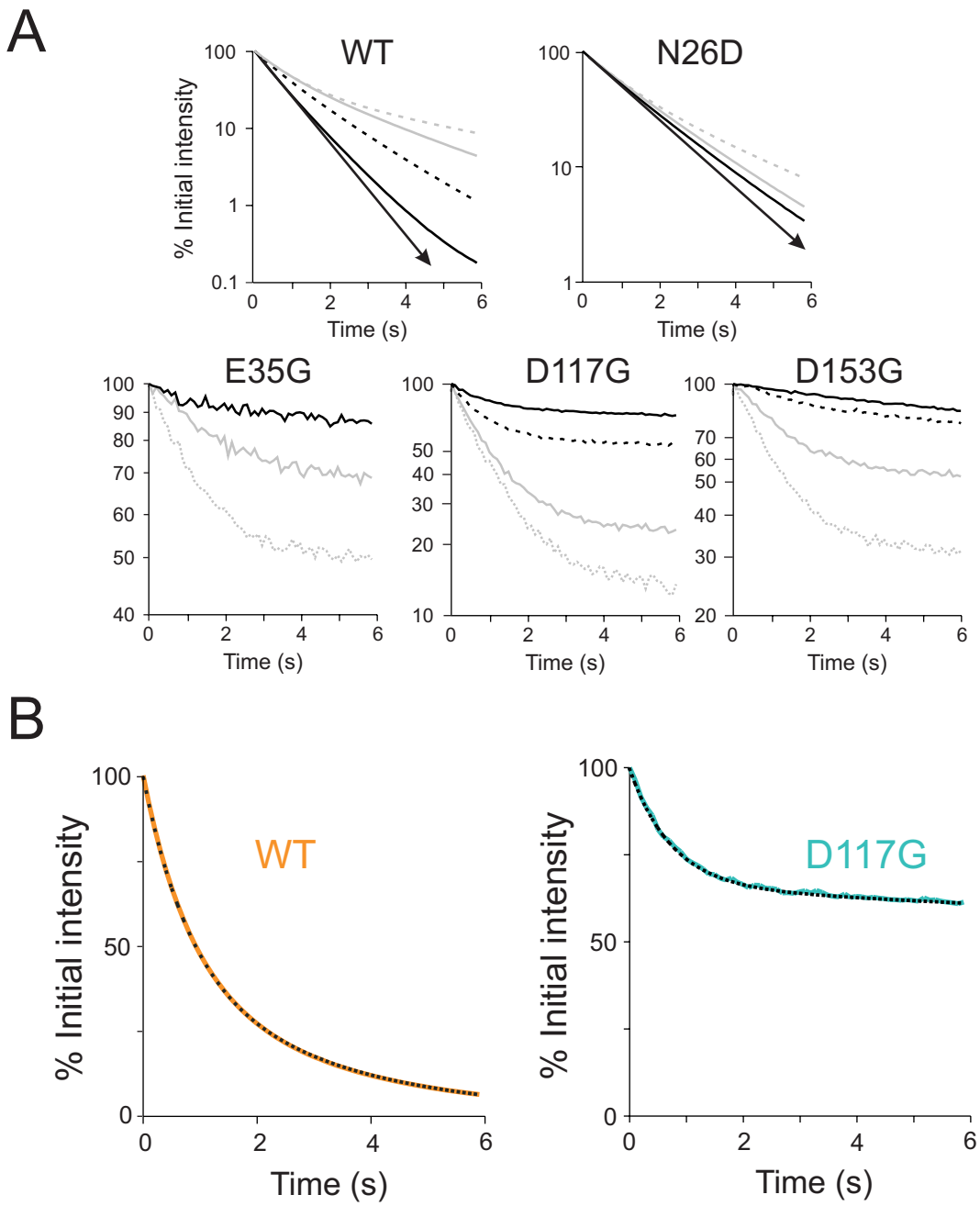

Supporting Figure 3

WT

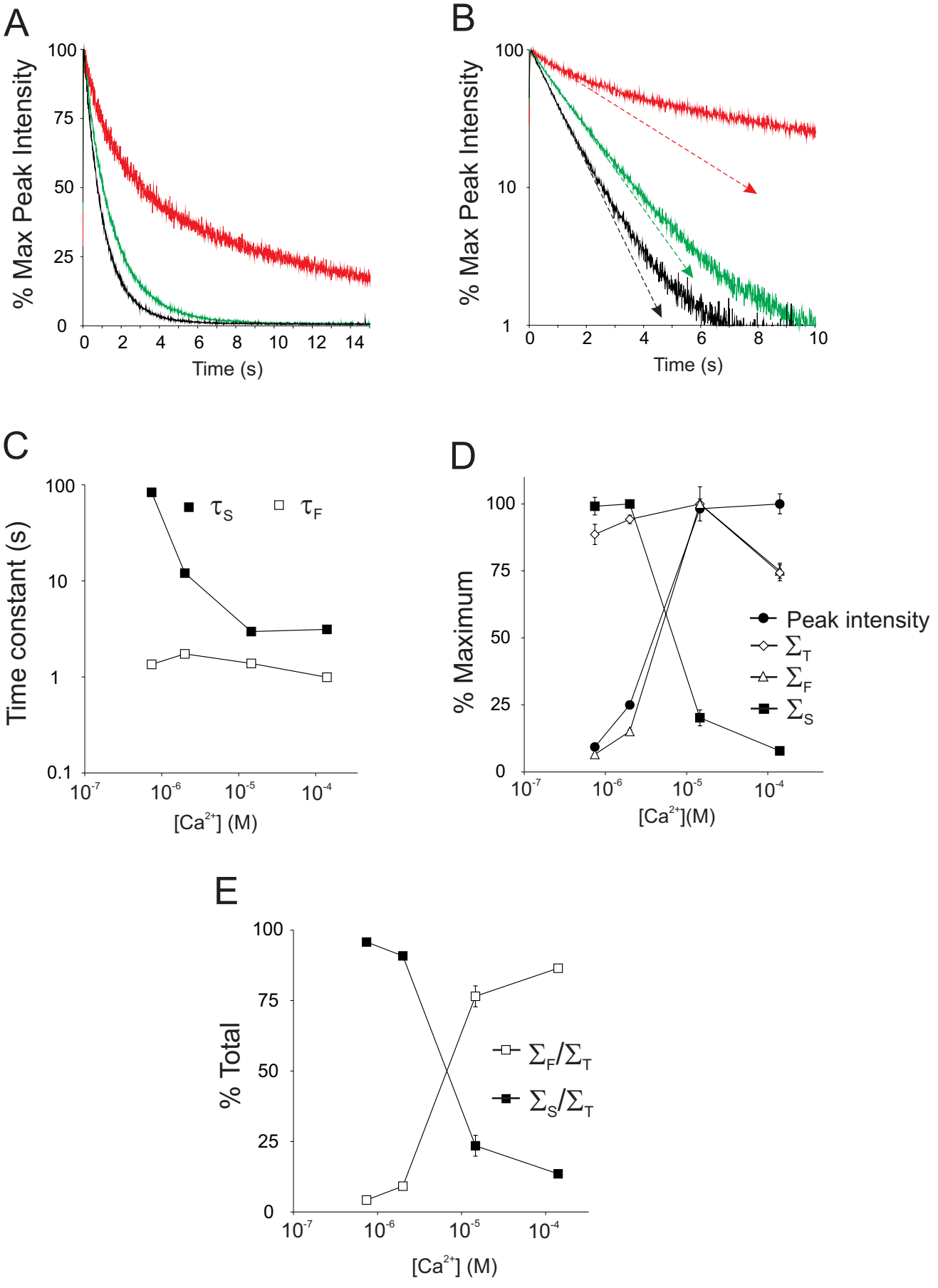

Supporting Figure 4

D153G

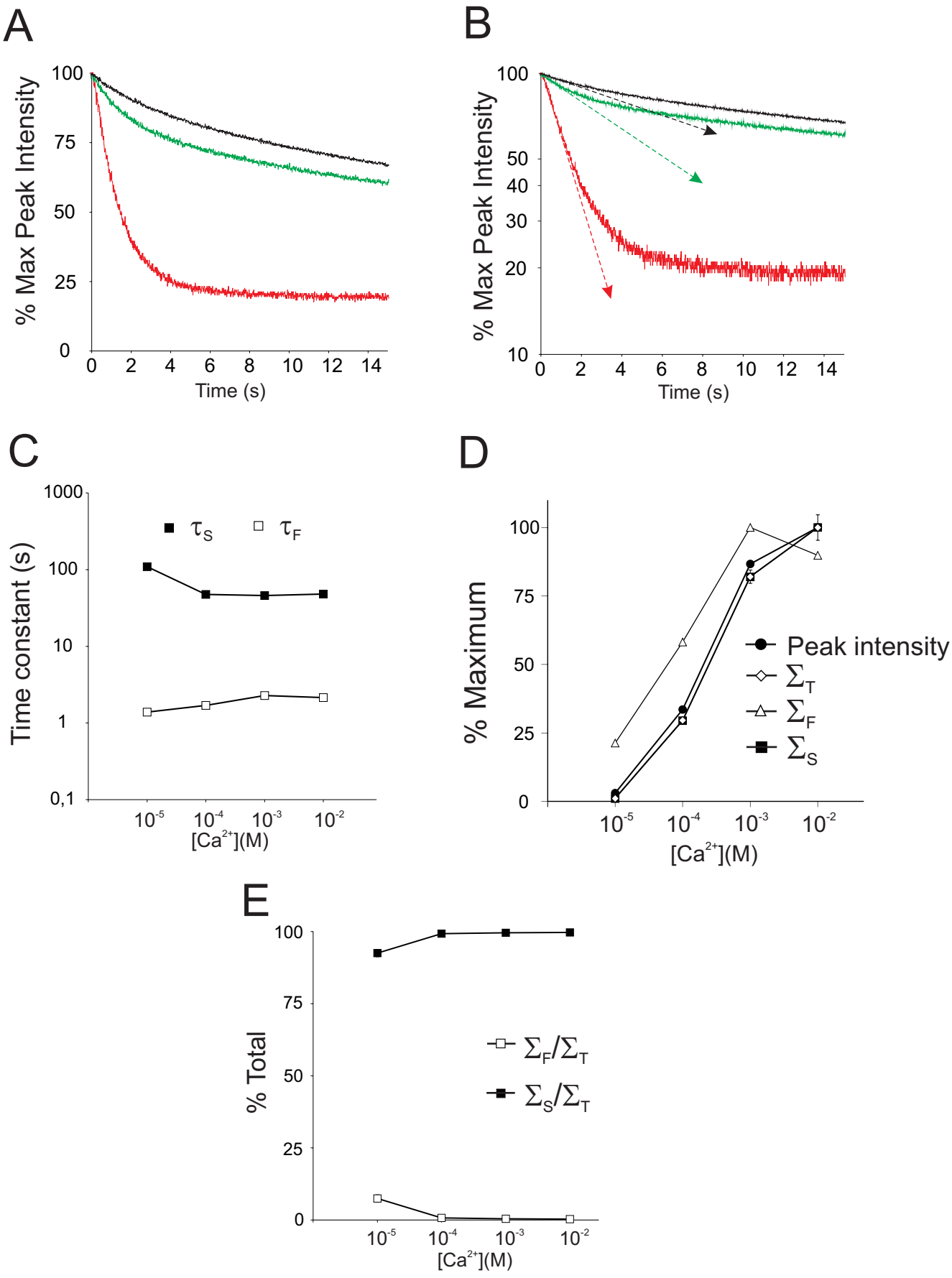

Supporting figure 5